

A space Fresnel Imager for ultra-violet astrophysics: example on accretion disks

Truswin Raksasataya · Ana-Ines Gomez de Castro · Laurent Koechlin · Jean-Pierre Rivet

Received: 14 November 2010 / Accepted: 16 March 2011 / Published online: 12 May 2011
© Springer Science+Business Media B.V. 2011

Abstract The Fresnel Diffractive Imager concept is proposed for space borne astronomical imaging at Ultra-Violet wavelengths, using diffractive focalization. The high angular resolution and high dynamic range provided by this new concept makes it an ideal tool to resolve circumstellar structures such as disks or jets around bright sources, among them, pre-main sequence stars and young planetary disks. The study presented in this paper addresses the following configuration of Fresnel diffractive imager: a diffractive array 4 m large, with 696 Fresnel zones operating in the ultra-violet domain. The diffractive arrays are opaque foils punched with a large number of void subapertures with carefully designed shapes and positions. In the proposed space missions, these punched foils would be deployed in space. Depending on the size of the array and on the working spectral band, the focal length of such imagers will range from a few kilometers to a few tens of kilometers. Thus, such space mission requires a formation flying configuration for two satellites around the L2 Sun-Earth Lagragian point. In this article, we investigate numerically the potential of Fresnel arrays for imaging circumstellar dust environments. These

T. Raksasataya · L. Koechlin (✉)

Laboratoire d’Astrophysique de Toulouse-Tarbes, Université de Toulouse, CNRS,
14 avenue Edouard Belin, 31400 Toulouse, France

URL: <http://www.ast.obs-mip.fr/koechlin>

A.-I. Gomez de Castro

Fac. de CC Matematicas, Universidad Complutense de Madrid, 28040 Madrid, Spain

J.-P. Rivet

Observatoire de la Côte d’Azur, Département Cassiopée, Université de Nice
Sophia-Antipolis, CNRS, B.P. 4229, 06304 NICE Cedex 4, France

simulations are based upon simple protostellar disk models, and on the computed optical characteristics of the instrument. The results show that protoplanetary disks at distances up to a few thousand parsecs can be successfully studied with a 4 m aperture Fresnel imager in the UV.

Keywords Circumstellar discs · Dust · High angular resolution · High dynamic range · Fresnel imager

1 Introduction

The Fresnel Diffractive Array Imager (FDAI) is based on the Fresnel Zone Plate concept [13]. It has been proposed in 2005 for space imaging [5, 6] and tested with laboratory breadboard designs [10, 11]. It is also described elsewhere in this special issue [2, 7, 9].

For the sake of self consistency of the present paper, we recall here some basic facts and formula related with Fresnel diffractive imagers. A Fresnel imager of aperture ϕ has a wavelength-dependent angular resolution:

$$R_{\text{airy}} = \frac{\lambda}{\phi}, \quad (1)$$

which is similar to that of a square aperture telescope of equivalent size. The focal length of a FDAO depends on the linear size ϕ of the array, on the wavelength λ , and on k_{\max} , the number of Fresnel zones from center to corner according to the following formula:

$$f = \frac{\Phi^2}{8k_{\max}\lambda} \quad (2)$$

For example, a “large” 20 m FDAO, with 2,000 Fresnel zones from center to corner will have a focal length of 66 km at 250 nm, and 140 km at 120 nm. A “small” 4 m FDAO with 700 Fresnel zones will have a focal length of 11 km at 250 nm, and 24 km at 120 nm.

For several reasons, FDAO’s are most valuable for UV imaging. First, the light is focused without any absorption or reflection loss (the focuser only involves void holes). Second, the light focused by a FDAO has a wave front quality which is independent of the wavelength. If the diffractive array is manufactured according to the desired specifications, the resulting image is diffraction-limited at all wavelengths. Thus, working with smaller wavelengths will increase the resolution limit without hampering the image quality. Furthermore, diffraction focussing provides high dynamic range that is otherwise difficult to reach in UV, and will allow to map disks around stars without having to use coronagraphs that simultaneously block the stellar radiation and the most interesting inner region of the disk.

As a consequence, protostellar disks around Pre-Main Sequence (PMS) stars are natural candidates for diffractive imaging studies. Indeed, intermediate mass (2–10 M_⊙) PMS stars, also known as Ae/Be Herbig (HAeBe) stars

have effective temperatures in the range 10,000–25,000 K and emit the bulk of their radiation in the UV domain. They are also significantly more luminous than solar-type PMS stars. High resolution and high dynamics images in the UV domain are likely to help understanding the structure and evolution of such objects.

In this article, we address some questions related to the observability of such stellar environments with space borne FDAI's. To be more specific, we present numerical simulations on how a FDAI configuration would render the structure of a protostellar disk. For this sake, we use standard stellar dust environment models, and compute the light intensity distribution which would result from stellar light diffusion within this dust (Section 2). Then, we compute the focal image a 4 m FDAI would produce from this light distribution (Section 3). Finally, conclusions are drawn about the observability of protostellar disks with UV space borne FDAI's (Section 4).

2 Disk models

Protostellar disks are angular momentum reservoirs generated during star formation to store the angular momentum excess associated with gravitational collapse of rotating clouds (see e.g. [15]). Disks are heated by the release of gravitational energy in the accretion process and also by stellar irradiation. The gravitational energy is mainly released in the disk midplane while the stellar radiation is absorbed through the atmosphere; this gives rise to a vertical temperature inversion over most of the disk and an “overheated” dusty atmosphere [1]. UV photons are absorbed in the dusty atmosphere (see [14]). Thus for this modelling we should only consider the UV radiation produced by the scattering of UV photons in the disk atmosphere, i.e., above one scale height in the disk.

In our first model: a standard α -Disk model, we assume an inner and outer disk radius of 0.2 AU and 1,000 AU respectively, and stellar masses $M = 0.5 M_{\odot}$, $1 M_{\odot}$ and $3 M_{\odot}$ as in Hayashi [3]. The dust is assumed to have uniform optical properties all over the disk: dust grains are assumed to be spheres of constant radius $a = 0.5 \mu\text{m}$, and mass $m_{\text{grain}} = 0.5 \cdot 10^{-15} \text{ kg}$. The local number density of dust grains is derived from the standard accretion disks mass distribution assuming a gas-to-dust mass ratio of 100.

2.1 Vertical density distribution in accretion disks

Following the standard model for α -accretion disk [8], the vertical distribution of matter is given by:

$$\rho(r, z) = \rho_0(r) \exp\left(-\frac{z}{H(r)}\right)^2 \quad [\text{g/cm}^3] \quad (3)$$

where r and z are the cylindrical coordinates of any given point in the disk, $\rho_0(r)$ is the matter density in the mid-plane at distance r from the star and

$H(r)$ is the vertical scale height. If the gravitational field is dominated by the star, the disk thickness can be readily derived as $H(r) = c_s(r)/\Omega(r)$ where $\Omega(r)$ is the Keplerian angular velocity of the material orbiting in the disk at a radius r :

$$\Omega(r) = (GM)^{\frac{1}{2}} r^{-\frac{3}{2}} = 2\pi \left(\frac{M}{M_\odot} \right)^{\frac{1}{2}} \left(\frac{r}{1 \text{AU}} \right)^{-\frac{3}{2}} [\text{yr}^{-1}], \quad (4)$$

and $c_s(r)$ is the local sound velocity:

$$c_s(r) = \sqrt{\frac{\gamma k_B T(r)}{\mu m_H}}. \quad (5)$$

Here, γ stands for the adiabatic index, μ is the mean molecular weight (2.34 as for a molecular H₂ disk) and m_H is the mass of a hydrogen atom. Consequently, a simple expression can be derived for $H(r)$, in terms of the disk temperature law $T(r)$:

$$H(r) = \left(\frac{\gamma r^3 k_B T(r)}{GM\mu m_H} \right)^{\frac{1}{2}} \quad (6)$$

The temperature in the mid-plane of an α -disk is given by:

$$T(r) = 127.8 \text{ K} \times \left(\frac{\dot{M}}{10^{-8} M_\odot/\text{yr}} \right)^{\frac{1}{4}} \left(\frac{M}{M_\odot} \right)^{\frac{1}{4}} \left(\frac{r}{1 \text{AU}} \right)^{-\frac{3}{4}} f(r) \quad (7)$$

where \dot{M} is the accretion rate, M_\odot and R_\odot are the solar mass and radius, respectively and $f(r) = \left(1 - \left(\frac{R_*}{r}\right)^{\frac{1}{2}}\right)^{\frac{1}{4}}$ which is $\simeq 1$ for $r > 0.4$ AU, which is the only relevant case for this study. Henceforth:

$$H(r) = 2.26 \cdot 10^9 \text{ m} \times \left(\frac{\dot{M}}{10^{-8} M_\odot/\text{yr}} \right)^{\frac{1}{8}} \left(\frac{M}{5 M_\odot} \right)^{-\frac{3}{8}} \left(\frac{r}{1 \text{AU}} \right)^{\frac{9}{8}} \quad (8)$$

2.2 Radial distribution of the column density

In steady accretion disks, the radial mass flow is constant and the disk surface density $\Sigma(r)$ is prescribed by the disk viscosity $\nu(r) = \alpha c_s(r) H(r)$ as follows:

$$\Sigma(r) = \frac{1}{\nu(r)} \frac{\dot{M}}{3\pi} f(r)^4 [\text{kg m}^{-2}] \quad (9)$$

Thus:

$$\Sigma(r) = 283.2 \text{ kg m}^{-2} \times \left(\frac{\dot{M}}{10^{-8} M_\odot/\text{yr}} \right)^{\frac{3}{4}} \left(\frac{M}{5 M_\odot} \right)^{\frac{1}{4}} \left(\frac{r}{1 \text{AU}} \right)^{-\frac{3}{4}}. \quad (10)$$

The density in the disk midplane can thus be approximated by:

$$\rho_0(r) = \frac{\Sigma(r)}{H(r)} \quad (11)$$

which yields, after some algebra,:

$$\rho_0(r) \simeq 12.5 \cdot 10^{-9} \text{ kg m}^{-3} \times \left(\frac{\dot{M}}{10^{-8} M_{\odot}/\text{yr}} \right)^{\frac{5}{8}} \left(\frac{M}{5 M_{\odot}} \right)^{\frac{5}{8}} \left(\frac{r}{1\text{AU}} \right)^{-\frac{15}{8}} \quad (12)$$

For a Ae Herbig star, fiducial values are: $\alpha = 0.01$, $M = 5M_{\odot}$, $\dot{M} = 10^{-8} M_{\odot} \text{ yr}^{-1}$.

2.2.1 Fiducial distribution of dust grains

Assuming a gas-to-dust ration of 100 and a The number density of dust grains, $N_d(R, z)$ is directly derived from $\rho(R, z)$ as follows:

$$N_d(R, z) = \frac{\rho(R, z)}{\eta m_d}$$

where η is the gas-to-dust mass ratio, and $m_d \simeq 0.5 \cdot 10^{-15} \text{ kg}$ is the mass of the dust grains. This yields:

$$N_d(r, z) = 2.5 \cdot 10^5 \text{ m}^{-3} \times \left(\frac{\dot{M}}{10^{-8} M_{\odot}/\text{yr}} \right)^{\frac{5}{8}} \left(\frac{M}{5 M_{\odot}} \right)^{\frac{5}{8}} \left(\frac{r}{1\text{AU}} \right)^{-\frac{15}{8}} \exp - \left(\frac{z}{H(r)} \right)^2 \quad (13)$$

with $H(r)$ given by Eq. 8. For more realism, we assume that the dust grain density vanishes for $r < R_{\text{in}} = 10 \text{ AU}$ (inner disk radius). Indeed, at the center of the disk is located the protostar (not represented in the images below), the strong radiation of which evaporates the dust grains located at distances smaller than the “inner radius” of the disk. The highest density of dust is found at distances just above the inner radius. At $r > R_{\text{out}} = 1,000 \text{ AU}$ (beyond outer disk radius), the dust density will be considered null.

2.3 Ray tracing

In our simplified model, we consider single light scattering by dust grains (no multiple diffusion). Thus, dust grains receive light from the star only, not from other parts of the illuminated disk. The disk volume is discretized into finite elements within an orthogonal coordinate system centered on the star with reference Z axis along the observers direction. The circulstellar disk plane is placed at an inclination i with regard to the X, Y (sky) plane. For each finite element, we compute the illumination received by dust grains from the star.

It is worth noting that not all points in the disk volume need to be considered, since the scattering of UV photons only occurs in the outer layers of the disk atmosphere, namely in the so-called “Photo Dissotiation Region” (PDR). The UV radiation is absorbed by H_2 molecules, leading to the formation of

a photodissociation front into the disk and leaving a photoevaporative flow behind.

The light intensity diffused towards the observer is computed according to the Henyey and Greenstein [4] diffusion model:

$$I_{\text{Scat}} = \frac{I_0}{r^2} \pi a^2 \phi(\theta) N_d(r, z) \quad (14)$$

where

I_{Scat}	scattered light intensity ($\text{W} \cdot \text{sr}^{-1}$).
I_0	incoming light intensity ($\text{W} \cdot \text{sr}^{-1}$).
a	radius of dust grain.
r	distance of dust from central protostar
θ	diffusion angle (see Fig. 1).
$\phi(\theta)$	diffusion factor.
$N_d(r, z)$	dust density.

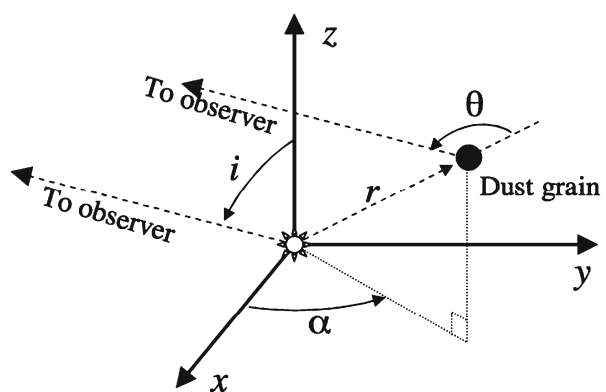
In this model, the diffusion factor (or scattering phase function) $\phi(\theta)$ is:

$$\phi(\theta) = \frac{1 - g^2}{4\pi \times (1 + g^2 - 2g\cos\theta)^{3/2}} \quad (15)$$

where g is the scattering phase function asymmetry. It varies from -1 to $+1$. When $g = -1$, all the incoming light is scattered back to the star. For $g = 0$, the light is diffused isotropically. For $g = +1$, the light goes forward “through” the dust grain as if it were fully transparent. The anisotropy factor g is wavelength dependent in the most general case. Here, we assume that it can be approximated to a constant value in the UV bandpass ($120 \text{ nm} < \lambda < 260 \text{ nm}$), and we have set it to an average value of $g = +0.6$ for the model presented.

We assume that no absorption occurs between the star and the dust grain, except in high dust density regions, where light is considered completely

Fig. 1 Illustrates the scattering of light by a dust grain at distance r from the star. θ is the diffusion angle. The observing direction lies in the (x, z) plane



blocked. From the dust grains to the observer, local absorption of the rays is taken into account, and a multiplicative transmission factor is applied locally.

We compute the local dust density in each volume element of our disk model, and from it we get a local absorption factor due to dust, that we apply to the rays traveling towards the observer. We consider the absorption by the dust grains only, computing it from their cross section and surface density in a given volume element. In the dense layers of the disk: when the UV transmission through the dust gets under 10^{-6} , we consider its contribution negligible and stop propagating the corresponding ray.

Finally, all the scattered radiation is integrated onto a plane perpendicular to the line of sight, so as to construct the 2D luminosity maps, which will be input to the Fresnel Imager. Considering absorption by dust only may overestimate the transmission of UV light, probably blocked before by the photodissociation front, but this simple model is not intended to give a fully precise image of protostellar disks: only to provide a base object for the assessment of performances of Fresnel Imagers.

To summarize, the parameters in Table 1 control this step of the process.

In Fig. 2, the dust disks are created by the model described in the above section, developed by ourselves and based on an irradiated α -disk model and the parameters in Table 1, left columns: respectively $0.5 M_{\odot}, 1 L_{\odot}$ —and $3 M_{\odot}, 10 L_{\odot}$.

In Fig. 3, the dust disk has been constructed as a set of nested ring-like structures whose physical parameters have been imported from the isodensity contour levels, using a numerical model based on Yorke and Bodenheimer [15]. The base parameters of this model are listed in Table 1, right columns: respectively $1 M_{\odot}, 1 L_{\odot}$ to account for a T-Tauri type star, and a $3 M_{\odot}, 10 L_{\odot}$ for a Herbig type central star. The disk is then projected onto the line of sight at different inclination angles, using a commercial ray tracing software.

As a result, frontier effects between surfaces are clearly apparent in Fig. 3. Also disk flaring produces dramatic external rings that are not observed in the

Table 1 Parameters used to simulate dust disks around young stars, projected on the line of sight and convolved by the PSF of a Fresnel imager, yielding the images in Figs. 2 and 3

	Fig. 2up	Fig. 2down	Fig. 3up	Fig. 3down	Unit
Stellar mass	0.5	3	1	3	M_{\odot}
Luminosity	1	10	1	10	L_{\odot}
Mass loss	10^{-8}	10^{-8}	10^{-8}	10^{-8}	M_{\odot}/year
α disk parameter	0.01	0.01	0.01	0.01	
Henyey–Greenstein param. for dust	0.6	0.6	0.6	0.6	
Disk inner radius	0.2	0.2	0.2	0.2	A.U.
Disk outer radius	1,000	1,000	1,000	1,000	A.U.
Distances from observer	1 & 10	1 & 10	1 & 10	1 & 10	kiloparsecs
Main Fresnel array aperture	4×4	4×4	4×4	4×4	m
Observation wavelength	121	121	121	121	nm
Angular resolution	0.07	0.07	0.07	0.07	"

Fig. 2 Images obtained by convolution of α -Disk models, placed at 1 kiloparsec, with the point spread function of a 4 m aperture Fresnel imager operating at $\lambda = 121$ nm. The field from left to right margin of the whole figure is 2.4 arc seconds. The disks parameters are in Table 3 *left columns*: a $0.5 M_{\odot}$ solar type T-Tauri star (*four top figures*), and a $3 M_{\odot}$ spectral type A (*four bottom figures*). The disks inclination angles from sky plane are 0° (*top left*), 60° (*top right*), 75° (*middle*), 90° (*lower*). The *arc shaped* limit visible at 0° and 30° is due to the external radius of all dust disk models in this figure, set to 1,000 AU. The luminosity scale has been square-rooted (except at 90°), to display the high dynamic range. The maximum brightnesses at 0° and 60° are much higher than at 75° and 90° (see Table 2)

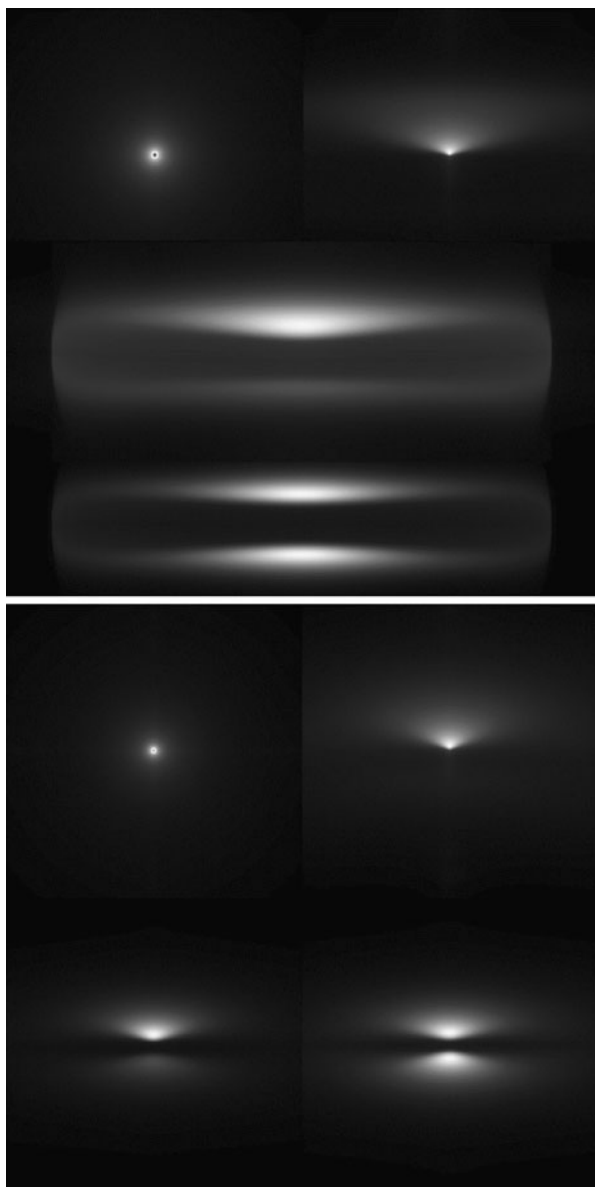
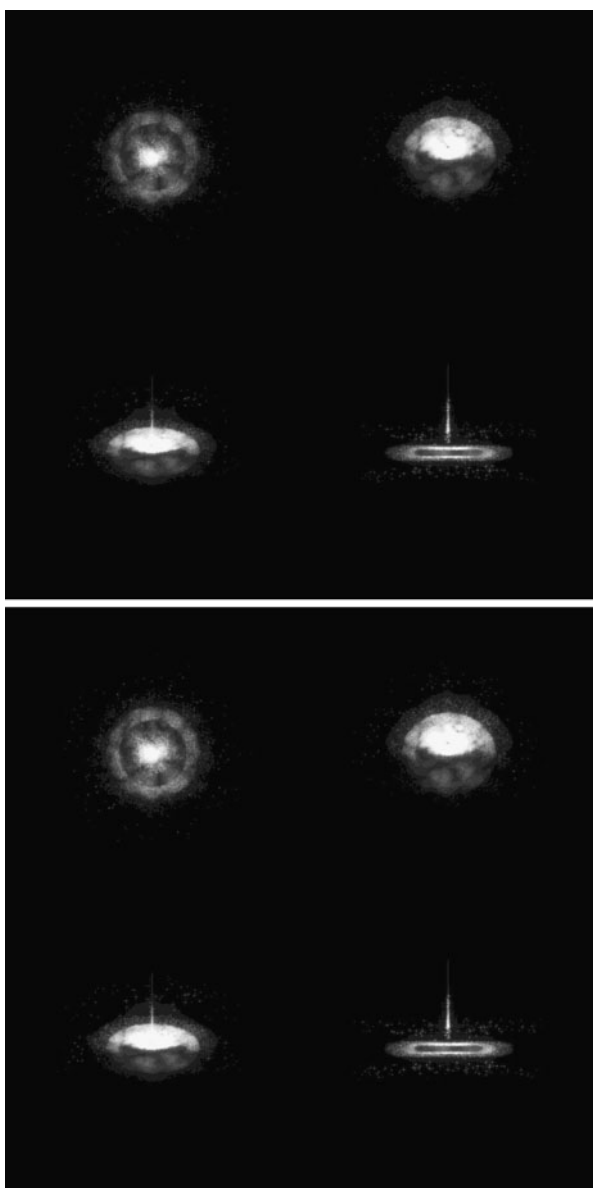


Table 2 Maximum disk brightness (arbitrary unit) as a function of inclination, for the α -Disk models shown in Fig. 2

Inclination	0°	60°	75°	90°
α -Disk $0.5 M_{\odot}$	541	54	6.1	3.1
α -Disk $3 M_{\odot}$	1,968	98	21	6.8

At low inclination angles from sky plane, there is in addition a very high brightness contrast between the inner and outer parts of the disks

Fig. 3 Images obtained by convolution of disk models with the PSF of the Fresnel imager: a protoplanetary disk of 135 UA mean radius, placed at a distance of 1 kiloparsec, seen with a 4 m aperture Fresnel array operating at $\lambda = 121$ nm. These disks are based on a model constructed as a set of nested ring-like structures (see text). Disk flaring produces external rings that are not observed in the standard accretion disk models, but seen around Fomalhaut. Disk model parameters are in Table 3, right columns: a $1 M_{\odot}$ solar type T-Tauri star (the four top images), and a $3 M_{\odot}$ spectral type A (the four bottom images). In both sets, the inclination angles are 0° , 30° , 60° , 90° from sky plane, left to right and top to bottom. The field from left to right margin of the whole figure is 2.4 arc seconds



standard accretion disk models. The objective of these tests is to analyze the sensitivity of Fresnel imagers to detect external ring and belts in the outer parts of the disk as the observed in Fomalhaut.

Although our disc models could be enhanced to take into account more complex mechanisms, and could be more precise, they are just used here

Table 3 Specifications for two possible Fresnel Space imagers

Specifications	Proposed Fresnel imager	Future large project
Array size	4 m	20 m
Fresnel zones	700	3,000
Field optics diameter	0.68 m	3 m
Bandpasses	120–150 and 200–260 nm	120–150 and 200–260 nm
Resolution at 121 nm	0.007"	0.0012"
Field at 121 nm	5.9"	4.5"

The 4 m configuration is proposed for the ESA “Cosmic Vision” call for 2020–2022 as a class “M” mission

for assessing the suitability of the instrument we propose to observation of protostellar disks at large distances.

3 Convolution and model perspective

The disk simulation code described above produces 2D “sky maps” of accretion disks. Whether or not all the details in these maps are revealed by the instrument depends on its capacities in resolution and dynamic range. To assess this, we convolve the 2D stellar disk maps with the point spread function (PSF) of a Fresnel imager. The following parameters control this step of the process:

- the distance at which the circumstellar disk is observed,
- the detailed PSF map, which will account for the dynamic range,
- the angular resolution: scale of the PSF map, obtained from aperture size and wavelength used.

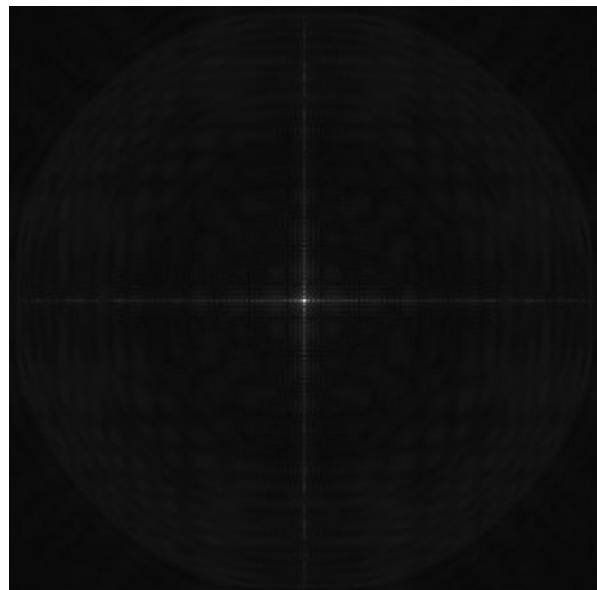
The PSF of the Fresnel imager is computed by a dedicated propagation software, developed by Serre [12], published elsewhere in this special issue. This software performs an end-to-end Fresnel propagation of a light wave through all the diffractive and refractive optical elements encountered on its way to the final image. It has been tested and validated by quantitative comparisons with optical PSFs of prototype Fresnel arrays.

The convolution of a circumstellar disk map by a PSF map yields the final simulated image. Having the dust disk models and the Fresnel imager PSF, we use an optical convolution code, developed by ourselves, to yield the images of dust disks that would be seen with a 4 m aperture Fresnel imager. The following parameters control the convolution step:

- scale of the PSF shown Fig. 4 (deduced from aperture and wavelength),
- distance of the protostar system.

This final step of calculation is what is presented in Figs. 2 and 3.

Fig. 4 Numerically computed Point spread function of the Fresnel array, and used for convolution of the disk models presented in this paper. The central lobe has a base radius of 0.007" for an aperture of 4 m and a waveband centered at 121 nm. It is displayed at power 0.25 in order to fit its high dynamic range and show the faint spikes



4 Conclusion

This work shows that with a 4 m aperture Fresnel array operating at 121 nm, protostellar disks up to distances of several kiloparsecs can be imaged with enough detail. This kind of instrument should be powerful tools to study the large variety of young stars and peculiar objects the Gould's Belt, at 140–160 pc, where prominent star forming regions such as Taurus, Lupus, and Ophiuchus are located. On a protoplanetary system close from us, such as Fomalhaut at 7.6 pc, a 4 m Fresnel imager would provide a linear resolution of 0.05 AU.

The Fresnel Diffractive Array Imager can be built in different configurations according to the science cases addressed, hence with various angular resolutions, dynamic ranges, and wavebands. As an example, the specifications in the left column of Table 3 are proposed for a mission to be launched around 2025: A 4 m Fresnel array at 121 nm, having an angular resolution of 7 milli arc seconds (mas) and yielding the images presented in Figs. 2 and 3.

The right column of Table 3 gives specifications for an ambitious project of further space mission, that would also be competitive in the visible and IR bands. Such a 20 m Fresnel array would allow to measure the inner radius of a circumstellar disk at 150 pc, down to 0.2 astronomical unit, and give many details on the structure and evolution of such disks. Stellar discs are just an example, many other science cases can be addressed with this new type of instrument.

Acknowledgements This work has been funded by Thales Alenia Space, Université de Toulouse, and CNRS, AIG research is supported by the Ministry of Education and Science of Spain through grant: AYA2008-6423-c03. We specially thank Denis Serre for letting us use the propagation code that he has developed and used for his Ph.D. work and his publications.

References

1. D'Alessio, P., Calvet, N., Hartmann, L., Lizano, S., Cant, J.: Accretion disks around young objects. II. Tests of well-mixed models with ISM dust. *Astrophys. J.* **527**(2), 893–909 (1999)
2. Deba, P., Etcheto, P., Duchon, P.: The Fresnel imager: preparing the way to space borne Fresnel imagers. *Exp. Astron.* (2011). doi:[10.1007/s10686-010-9202-5](https://doi.org/10.1007/s10686-010-9202-5)
3. Hayashi, C.: Structure of the solar Nebula, growth and decay of magnetic fields and effects of magnetic and turbulent viscosities on the Nebula. *Prog. Theor. Phys. Suppl.* **70**, 35–53 (1981)
4. Henyey, L.G., Greenstein, J.L.: Diffuse radiation in the galaxy. *Astrophys. J.* **93**, 70–83 (1941)
5. Koechlin, L., Serre, D., Duchon, P.: High resolution imaging with fresnel interferometric arrays: suitability for exoplanet detection. *Astron. Astrophys.* **443**, 709–720 (2005)
6. Koechlin, L., Serre, D., Deba, P., Pelló, R., Peillon, C., Duchon, P., Gomez de Castro, A.I., Karovska, M., Dézert, J.-M., Ehrenreich, D., Hebrard, G., Lecavelier Des Etangs, A., Ferlet, R., Sing, D., Vidal-Madjar, A.: The Fresnel interferometric imager. *Exp. Astron.* **23**, 379 (2009)
7. Koechlin, L., Rivet, J.P., Deba, P., Rakasataya, T., Gharsa, T., Gili, R.: Fresnel imager tetbeds: setting up, evolution, and first images. *Exp. Astron.* (2011). doi:[10.1007/s10686-011-9213-x](https://doi.org/10.1007/s10686-011-9213-x)
8. Lynden-Bell, D., Pringle, J.E.: The evolution of viscous discs and the origin of the nebular variables. *Mon. Not. R. Astron. Soc.* **168**, 603–637 (1974)
9. Koechlin, L., Rivet, J.-P., Deba, P., Rakasataya, T., Garsa, T., Gili, R.: Generation 2 testbed of Fresnel imager: first results on the sky. *Exp. Astron.* (2011). doi:[10.1007/s10686-010-9203-4](https://doi.org/10.1007/s10686-010-9203-4)
10. Serre, D.: L'Imageur interférométrique de Fresnel: un instrument spatial pour l'observation à haute résolution angulaire. PhD thesis, Université Paul Sabatier, Toulouse, France (2007)
11. Serre, D., Deba, P., Koechlin, L.: Fresnel interferometric imager: ground-based prototype. *Appl. Opt.* **48**(15), 2811–2820 (2009)
12. Serre, D.: The Fresnel imager: instrument numerical model. *Exp. Astron.* (2011). doi:[10.1007/s10686-010-9200-7](https://doi.org/10.1007/s10686-010-9200-7)
13. Soret, J.-L.: Sur les phénomènes de diffraction produits par les réseaux circulaires. *Arch. Sci. Phys. Nat.* **52**, 320–337, (1875)
14. van Zadelhoff, G.J., Aikawa, Y., Hogerheijde, M.R., van Dishoeck, E.F.: Axi-symmetric models of ultraviolet radiative transfer with applications to circumstellar disk chemistry. *Astron. Astrophys.* **397**, 789 (2003)
15. Yorke, H.W., Bodenheimer, P.: The formation of protostellar disks. III. The influence of gravitationally induced angular momentum transport on disk structure and appearance. *Astrophys. J.* **525**, 330–342 (1999)